

Nanophotonic Biosensors Within Lab on Chip Optical Systems

Daniel Hill

UMDO, Institut de Ciència dels Materials, Universitat de València, Catedrático José Beltrán, Paterna, Spain

Keywords: Nanophotonics, Slot-Waveguides, Ring Resonators, Porous Silicon, Biosensing, Lab-on-Chip, Birefringence, Quantum Dots.

Abstract: For ring resonator based sensors, volumetric limits of detection (LoD) of 5×10^{-6} RIU and 8.3×10^{-6} RIU (refractive index units) for sensitivities of 246nm/RIU and 2169nm/RIU were reported from FP6 SABIO (at 1.31 μ m) and FP7 InTopSens (at 1.55 μ m) respectively. These compare well to the state of art of 7.6×10^{-7} RIU for a sensitivity of 163 nm/RIU, as does the porous alumina based membrane sensors in FP7 Positive with their LoD of 5×10^{-6} RIU. More interestingly for the membrane sensors, the standard deviation of their measured values was below 5% and their flow through design with lateral distances to the sensor surface less than a diffusion length permit fast response times, short assay times and the use of small sample volumes (< 100 μ l). For protein binding recognition, within SABIO a surface LoD of 0.9 pg/mm² for anti-BSA on a gluteraldehyde-covered surface was recorded, corresponding to a 125ng/ml anti-BSA solution, whilst in InTopSens 5pg/mm² and 10ng/ml for biotin on a streptavidin coated surface was seen. For an assay of β -lactoglobulin - anti- β -lactoglobulin - anti-rabbit-IgG –streptavidin conjugated CdSe quantum dots the Positive sensors demonstrated a noise floor for individual measurements of 3.7ng/ml (25pM) for total assay times of under one hour.

1 INTRODUCTION

Increasing demands for rapid, reliable and economical near patient or in the field testing has led to strong and growing trend towards in-vitro point of care (PoC) sensing for clinical diagnosis, food safety, environmental monitoring, safety and security (Fan et al., 2008) (Hill, 2011). The demands for PoC sensing that can be used, such as by a single medical practitioner or in a remote field crop-testing environment, are driven by their facilitation of a massive socio-economic impact from the general improvement of quality of life they would bring. PoC sensing is enabled through the scaling of analytical chemical and biological instruments down to a single chip (Janasek et al., 2006) leading to: automation of the analysis, increased mobility of the instrument, shorter response times, reduced manual sample handling, and a low cost per test. Typical requirements for assay requirements consists of the reliable and selective identification of extremely low concentrations of biomarkers (infectious agents, pesticides, cardiac markers, allergens etc.) from other matter within small volumes of complex matrices (e.g. whole blood, sputum swabs, faeces, cell

lysate...) within a few minutes. Furthermore, it should have a commercially viable cost and be useable by a relatively unskilled operator outside of a lab environment. PoC in-vitro diagnostic devices are therefore required to provide fast, sensitive and selective analysis of assays, ideally in a parallel format and therefore of a technology that permits the fabrication of a high density of sensor ‘spots’ per chip area, as well as negating the need for lengthy off-chip sample preparation, all at an acceptable cost. To that end, many of the new approaches that have been explored are based on highly integrated sensors within a Lab on Chip format (Ligler et al., 2009).

At the core of these devices is the biosensor (Brecht et al., 1995) and those based on optical interrogation offer important advantages such as: 1) non-invasive, safe and multi-dimensional (intensity, wavelength, phase, polarization) detection; 2) well-established tools from communication and Micro-Nano technologies (MNT) industries (lasers, detectors, waveguides) and 3) optical frequencies that coincide with a wide range of physical properties of bio-related materials.

Refractive index (RI) sensing is often used in real-time monitoring of chemical processes and, when used with separation techniques such as liquid

chromatography or capillary electrophoresis, universal solute detection systems can be created (Markov et al., 2002). Within LoC devices, silicon nanophotonics has found much use recently as affinity sensors (Zinoviev et al., 2008) as the RI of aqueous macromolecular solutions is linear with macromolecule density (De Feijter et al., 1978) and so the mass of bound macromolecules, such as proteins, DNA, peptides, to a waveguide can be derived from measurements of the surface evanescent field. The commercially successful surface plasmon resonance (SPR) based sensors (Brecht et al., 1995) are such an example. Furthermore, the nanophotonic sensors can be economically mass-produced in a highly integrated format by using the same waferscale microfabrication technologies as those used for electronic microchips. Thus, to bring the powerful tool of highly integrated and reliable sensing into the hands of a wider user base, there is a *strong interest in integrating nanophotonic sensors into LOC platforms* for PoC applications. In this paper we compare various nanophotonic transducers from three EC funded projects (FP6 SABIO, FP7 InTopSens and FP7 Positive) that due to their small footprints and ease of integration with other on-chip optical and fluidic functions are particularly interesting as sensors for LoC devices. In doing so, we also compare them to the state of art for each technology type to fully put their advances into perspective.

2 SABIO

2.1 SABIO Nanophotonic Sensors

Optical ring resonators consist of a set of waveguides with at least one being a closed loop that is coupled to some sort of light input and output, conceptually analogous for light to acoustic whispering galleries. When light of the resonant wavelength is passed through the loop from input waveguide, it builds up in intensity over multiple round-trips due to constructive interference and is output to the output bus or detector waveguide which serves as a detector waveguide. The ring acts as a filter with its finesse determining how many select few wavelengths will be at resonance within the loop and its quality factor to how lossless it is. Researchers have been studying them since the 1980s (Tiefenthaler et al., 1984) (Lukosz et al., 1988) (Tiefenthaler et al., 1989) and inspired by Almeida et al's demonstration (Almeida et al., 2004) (Xu et al., 2004) of slot waveguides in

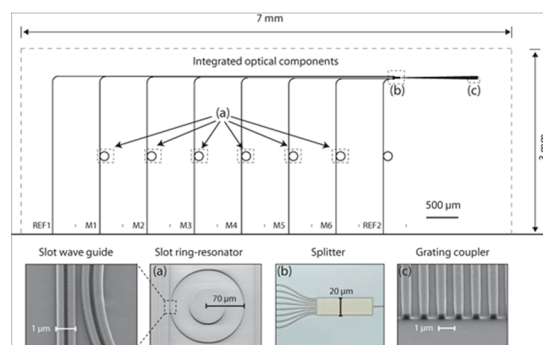


Figure 1: A top view of the layout of the nanofabricated SABIO optical chip (occupying a 3x7mm² area): Light is injected at the surface grating coupler (C) and split, by the multi-mode interference splitter (B), to the six sensing channels M1–M6 and the two reference channels REF1 and REF2. Inset are an optical micro-graph of the splitter (B); and electron micro-graphs of the grating coupler (C), and a slot-waveguide ring resonator (A), with an enlargement of the coupling region.

2004 the SABIO project targeted the implementation of these in a ring resonator format for biosensing. Si planar waveguide ring resonators, and even more so slot-waveguides ring resonators are very attractive for biosensing due to their small footprint, high Q-factors, and compatibility with on-chip optics and microfluidics (Sohlström et al., 2010). Their design permits parallel sensor operation which not only yields higher throughput by multiple analyses of one sample, or simultaneous analyses of multiple samples, but it can also provide reference channels for drift compensation and control experiments. Such reference measurements are particularly important for automated labs-on-chips without temperature stabilization. In SABIO the optical chip (Figure 1) was designed with 6 measurement channels and two reference channels, and channel to slot-mode converters were used for conversion between the two waveguide types before and after the ring resonator coupling regions, where the bus slot-waveguides have rail widths of 400 nm and a slot width of 200nm.

The coupling gap was 350 nm and in the sensing ring, asymmetric slot-waveguides with the inner rail widened to 550 nm were used for high optical confinement and low bending loss. Details of the choice of low pressure chemical vapour deposition (LPCVD) silicon nitride on thermally oxidized silicon wafer technology, as well as general design rules for the chip, that led to measurements being able to be made over a 7K operating window, without external temperature control and individual sensor calibration (Gylfason et al., 2010), are beyond the scope of this paper.

2.2 SABIO Measurements and Discussion

In determining the volumetric RI sensitivity and limit of detection for the SABIO chips, sensing experiments were performed using a dilution series of ethanol and methanol plugs in a running buffer of deionized (DI) water. Full details of the sensing experiments (Carlborg et al., 2010) are beyond the scope of the paper including how a fitting algorithm was used to determine more accurately the positions of the drips in the ring characteristics, pushing down the wavelength noise significantly to below the laser-tuning step and the use of reference channels with DI water to correct for drift. At 1300nm, an index sensitivity of $S_n=246$ nm/RIU was measured and the sensor resolution (R) taken as 1.2pm, following the convention of 3 standard deviations σ of the total system noise, with the volumetric RI LOD given by $L_n=R/S_n$ and thus 5×10^{-6} RIU.

The SABIO chip's performance as a surface mass sensor was studied by measuring the binding of anti-bovine serum albumin (anti-BSA), injected in increasing concentrations in a running buffer of phosphate buffered saline (PBS), to a surface selectively activated by a layer of the molecular linker glutaraldehyde. From a saturation induced resonance shift estimated at $\Delta\lambda=2.55$ nm, with a surface density of a monolayer (σ_p) of anti-BSA measured at 2.0 ng/mm² by dual polarisation interferometry (DPI) with the Farfield AnaLight 4D system, a mass sensitivity, or $S_m=\Delta\lambda/\sigma_p$ of $S_m=1.3$ nm/(ng/mm²) was measured. The surface mass detection limit, $L_m=R/S_m$, where R is the sensor resolution, was determined at 0.9pg/mm² corresponding to a concentration of 125ng/ml anti-BSA in PBS solution.

The detection limits of 5×10^{-6} RIU for volume sensing and 0.9 pg/mm² or 125ng/ml for protein binding, compare favorably to other published ring resonator results. These are primarily due to the use of multiple transducers on the chip to compensate for external disturbances, the high sensitivity of the slot-waveguide ring resonators and the low system noise of 1.2 pm from fitting an analytical model to the spectrum, effectively due to utilizing all the information available (Kazmierczak et al., 2009). As seen ahead, this is in contrast to the approaches used in the later projects InTopSens and Positive, neither of which used a non-directly mass fabrication compatible technology such as electron beam lithography.

3 InTopSens

3.1 InTopSens Nanophotonic Sensors

Whereas the SABIO application required a chip design with 6 ring resonator sensors, 64 were required for the InTopSens application and therefore a far smaller footprint per sensor. A starting point for sensor development was therefore silicon-on-insulator (SOI) ring resonators due to their higher index contrast than those based on silicon nitride and therefore potentially a higher degree of integration. Moreover, they had previously demonstrated (De Vos et al., 2007) a volumetric RI sensitivity of 70 nm/RIU and LOD of 1.3×10^{-5} RIU as well as a LOD of 7ng/ml for protein binding (biotin-avidin) recognition. Therefore for a suitably high degree of integration, with an equal or better LoD, slot-waveguide racetrack resonators with 100nm wide slots in SOI were nanofabricated (Claes et al., 2009), with footprints of just 13 μ m x 10 μ m, using the mass fabrication-compatible optical lithography, opening the way toward cheap, disposable chips in contrast to the SABIO ring resonators.

3.2 InTopSens Measurements and Discussion

Using aqueous salt solutions volumetric sensing experiments with these SOI slot ring resonators, demonstrated a refractive index sensitivity of 298 nm/RIU and a LOD of 4.2×10^{-5} RIU (Figure 2). As the sensitivity value lies within a range of theoretical values from an empty slot to a liquid filled slot it demonstrates that liquid has penetrated the narrow slot region.

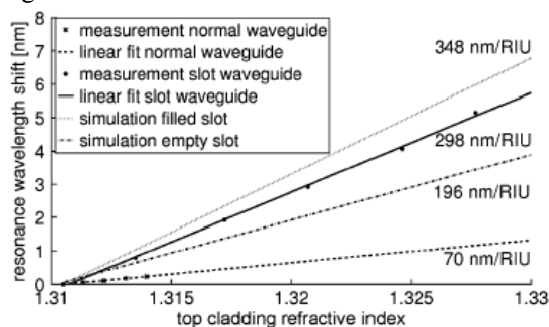


Figure 2: A comparison between the experimental resonance wavelength shift of a normal-waveguide based ring resonator and the theoretical and experimental resonance wavelength shift of a slot-waveguide based ring resonator for top refractive index.

After silanizing the sensor surface protein binding experiments (biotin-avidin recognition) showed a limit of detection of 10ng/ml (Claes et al., 2009), or 5pg/mm². The saturation shift was 3.5 times that of the SABIO device, lying between the theoretical values for avidin binding only outside of the slot and for it lying both inside and outside of the slot. Thus, although it demonstrated that surface chemistry for selective label-free sensing of proteins can be applied inside a 100 nm wide slot region for a smaller footprint slot waveguide sensor, it also showed a poorer LoD compared to the SABIO device. Principally the poorer LOD was due to a lower resolution or quality factor mostly caused by bending and mismatch losses although sidewall inclination, roughness from silicon's greater sensitivity to nanofabrication limitations, the presence of a biochemical layer, and absorption also contributed.

In an aim to improve the LoD whilst maintaining a small footprint other ring resonators were fabricated whose designs were based on modifications to existing (slot) ring resonator waveguide sensors such as:

- The use of notch ring resonator filters instead of add-drop filters
- Increasing the sensor circumference
- Switching to 1300nm where water is less absorbent
- Combining quasi-TE and quasi-TM modes

One such ring resonator demonstrated a volumetric limit of detection of 5×10^{-6} RIU through aqueous salt solution sensing experiments and an improved surface mass LOD of 2pg/mm² for protein binding (biotin/avidin) experiments corresponding to 10ng/ml. Another was based around the use of the Vernier effect through suitably designed cascaded ring resonators that were folded to permit high integration. For these (Claes et al., 2010), aqueous salt solution sensing experiments demonstrated a volumetric sensitivity of 2169nm/RIU and a limit of detection of 5×10^{-6} RIU, equal to that of the larger SABIO sensors, promising a favourable protein binding limit of detection.

4 POSITIVE

4.1 Positive Nanophotonic Sensors

Planar nanophotonic sensors such as those in SABIO and InTopSens have demonstrated LODs that meet the criteria of analyte concentration measurements for many applications. However, although some require lower LoDs still, many sensors, including those in

SABIO and InTopSens, are far from becoming a reality within commercial PoC diagnostic platforms for other reasons. These include poor planar integration, high fabrication costs, but most importantly a slow time to response and subsequently long times to assay result as well as the need for large sample volumes and subsequently expensive reagents. For example in both SABIO and InTopSens the time taken to go from steady state concentration to another was over 40 minutes and therefore assays took typically far in excess of an hour whilst response times to an analyte and/or reagent injection into their microfluidic systems were typically in excess of 5 minutes. Furthermore, whilst SABIO and InTopSens sensors required millilitres of blood, along with millilitres of costly reagents, applications that test young children can be limited to the ~100 μ l of blood taken by finger prick collection. All of these deficiencies in both of these projects, and many others, are due to the use of 2D or planar sensors and the long path lengths of the analytes to their surfaces relative to their diffusion lengths, arising from the common use of lateral flow geometry in sensor cartridge design.

Nanostructured materials like porous silicon (PSi) or porous alumina (AAO) have however recently gained special attention for sensing, due to their 3D design allowing higher surface areas per unit planar area for capturing analytes than planar biosensors, permitting lower detection limits (Lazzara et al., 2011) and higher integration of assays. Due to the use of reflectometric interference spectroscopy (RIS) however, optical biosensors based on porous membranes (Orosco et al., 2009) (Tsang et al., 2012) (Alvarez et al., 2009) (Kumeria, Kurkuri et al., 2012) can have their pores only open at one end and the diameters of those limited to 100nm to avoid light scattering (Kumeria & Losic, 2012). With that structure, the delivery of the analytes into the pores is therefore mainly governed by the stationary flux produced by electrostatic interactions, resulting in slow responses and so long sensing times.

The choice of a porous membrane based biosensor in the FP7 Positive project was based on the constraints of its application that required the detection of 16 different proteins found in concentrations of 0.24ng/ml upwards in serum sample volumes of 100 μ l samples within 15 minutes of their introduction into the instrument. In order to meet all of the application criteria, freestanding macroporous AAO membranes with 200 nm pore diameters were used, to allow analyte molecules to flow-through the pores less than a diffusion length from the assay surface on the pore walls, breaking the

mass transport limitations (Yanik, 2010) (Guo, 2011), and so effectively targeting their delivery, for real-time biosensing responses.

With the pores of macroporous AAO membranes perpendicular to their planar surface, any induced birefringence is very sensitive to the refractive index of the material within the pores (Alvarez, 2011) (Alvarez, 2012), and this was used as a sensing mechanism (Alvarez, Sola et al., 2013) in an optical polarimetry based experiment (Figure 3).

In the experiment, the AAO pore walls within the membrane were functionalized with an epoxysilane before being spotted with β -Lactoglobulin protein and the binding first of rabbit anti- β -lactoglobulin and then a secondary antibody anti-rabbit Immunoglobulin G was monitored in real-time. The membrane itself is affixed with a 1 μ m thick layer of PMMA (Poly(methyl methacrylate)) resist to a 500 μ m thick 15 by 15 mm piece of single side polished silicon wafer support, with a 750 μ m diameter opening (Figure 4). Prior to the biosensing experiment, a bulk refractive index sensitivity of 5.2×10^{-6} refractive index units was measured from signal responses to different concentrations of NaCl solutions for the mounted membranes within a flow cell.

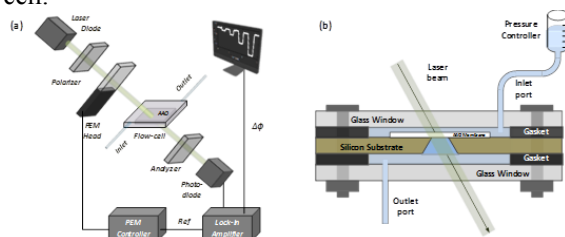


Figure 3: (a) Layout of the optical polarimetric readout platform used for measuring the phase retardation within the membranes from phase locked loop measurements using a 980nm laser diode. (b) Scheme of fluidic setup integrated within a flow-cell where the mounted membrane is placed and whose inlet port is connected to a pressure controller providing a constant pressure flow.

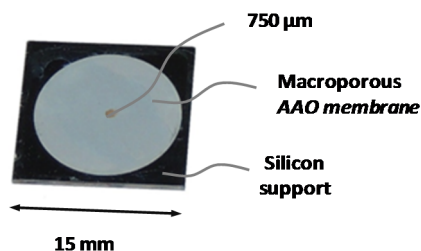


Figure 4: Picture of a freestanding membrane mounted on a silicon support.

4.2 Positive Measurements and Discussion

Recently this approach was repeated for immunosensing (Alvarez 2014), by coating the membrane with a functional copolymer, copoly(DMA-NAS), through a novel procedure that has demonstrated less non-specific binding, and therefore greater selectivity, and more stability over time for immobilized allergens than epoxysilane (Platt, 2014). Specifically this polymer was previously demonstrated to immobilize allergens on different materials, such as glass, nitrocellulose, silicon (Cretich, 2010) and more recently on a SiO_xNy DPI chip (Platt, 2014), whilst allowing an efficient measurement of their interactions with allergen-specific Immunoglobulin E (IgEs) in complex matrices of serum, proving its suitability as a non-fouling coating and that it is robust to allergen storage.

Prior to the immunosensing experiments in order to obtain both the bulk sensitivity, and its reproducibility a series of bulk refractive index experiments with the polarimetry setup were carried out (Sola, 2015), on ten different copolymer functionalized macroporous alumina membranes, with an allergen immobilized on the pore surfaces (Figure 5), on silicon supports and mounted within a flowcell. Briefly, after purging with CO₂, PBS-T (PBS, 0.02% (v/v) Tween 20) was flown through the membranes for fifteen minutes in order to obtain a base line, before flowing four solutions of NaCl in PBS with concentrations ranging from 0.2% (m/v) to 2% (Figure 6).

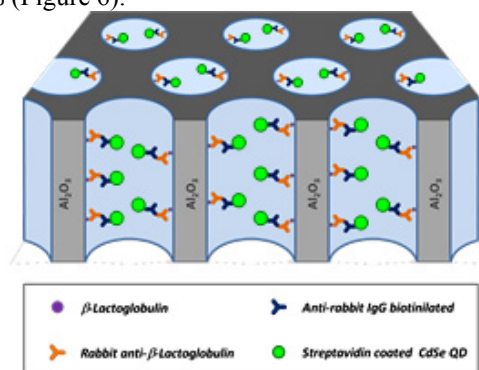


Figure 5: The immunoassay carried out in a macroporous alumina membrane. β -lactoglobulin protein was used as the immobilized antigen for the detection of rabbit anti- β -lactoglobulin. Biotinylated secondary antibody (anti-rabbit-IgG) and streptavidin coated CdSe quantum dots were used to increase the signal produced by the primary antibody.

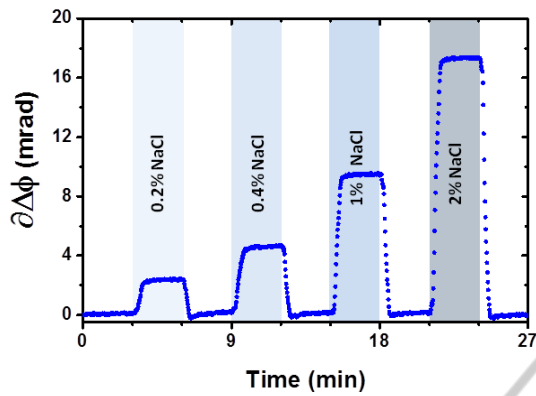


Figure 6: A sensorgram showing the signal response from flowing several solutions of various concentrations of NaCl in deionized water through a macroporous AAO membrane.

Measured polarimetric responses for all membranes when fitted with a linear curve gave a mean sensitivity of 5.2 rad RIU^{-1} (rad RIU^{-1}) with a standard deviation equal to 0.2 rad RIU^{-1} (Figure 7) which is $\sim 4\%$ of the average sensitivity value (which envisions a good reproducibility for these membranes, a necessity for a commercial device). This corresponds to a LoD of $5 \times 10^{-6} \text{ RIU}$ from a measurement system resolution of $2.7 \times 10^{-5} \text{ rad}$ (Alvarez, Serrano et al., 2013). Thereafter, each immunosensing experiment began by first introducing a running buffer of PBS-T for 15 minutes. In a first experiment the activity of the immobilized allergens were tested (Figure 8) using concentrations of $1 \mu\text{g/mL}$ (6.7 nM) for the first and secondary antibody and a concentration of 2.5 nM for streptavidin coated CdSe quantum dots (SA-QD). Firstly, the baseline obtained during the buffer rinse showed good stability, demonstrating that the antigen is stably immobilized on the polymer coated surface.

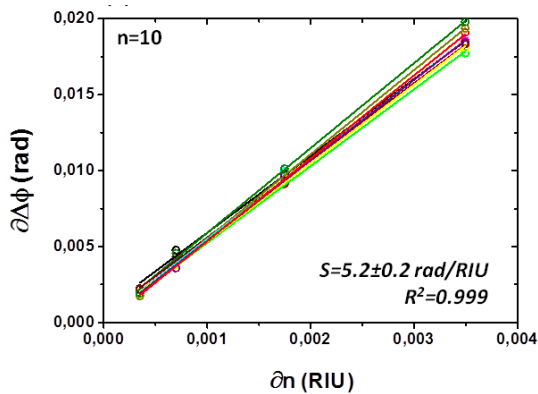


Figure 7: Overlaid phase retardation changes for ten different alumina membranes as a function of refractive index changes from different NaCl solutions.

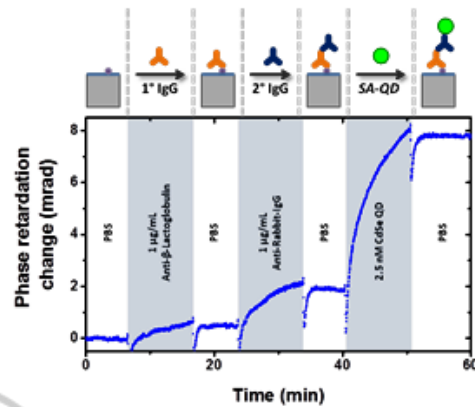


Figure 8: A sensorgram showing the signal response due to the binding of the first and secondary antibodies, followed by the SA-QD.

After recording a stable baseline during six minutes the first antibody rabbit anti- β -lactoglobulin was injected during 10 minutes, followed by a six minute rinse with the running buffer before the secondary antibody anti-rabbit IgG was injected during 10 minutes. As the secondary antibody is polyclonal, a larger response is observed for this, compared to the binding of the initial primary antibody. After further rinsing, the SA-QDs were added as a signal enhancer at a concentration of 2.5 nM , which was sufficient to saturate the captured secondary antibodies. Due to the size of the SA-QDs an enhancement of 5 times is observed in the signal over the response produced by the secondary antibody. Each sandwich assay, employing both a secondary and tertiary binding, took less than one hour reducing assay time fivefold and analyte

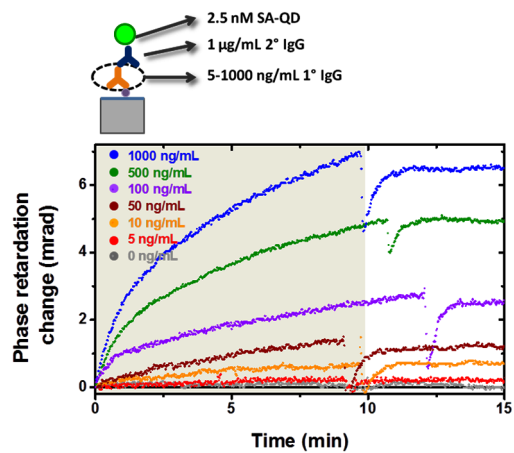


Figure 9: An overlay of the signal responses produced by the SA-QD when the concentration of the first antibody is increased from 5 ng/mL to 1000 ng/mL .

consumption by three orders of magnitude compared to biosensors based on porous membranes in flow-over configurations (Tsang, 2012). From measurements (Figure 10) a LoD was calculated at 33.7ng/ml (225pM). The reductions in assay time, sample and reagent volumes as well as response time are clearly advantages that result from the use of a flow through mechanism with analyte path lengths to the sensor walls less than a diffusion length, and a parameter related to these values is the capture efficiency. This was determined (Sola, 2015) by the use of a fluorescent flow-through capture assay using Cy3 labelled streptavidin which, when combined with modelling (Figure 11), was also used to provide pore size distribution information for the AAO membranes. Compared to a conventional planar biosensors, they show much higher efficiency for analyte capture from solution (17% vs 32%), which is

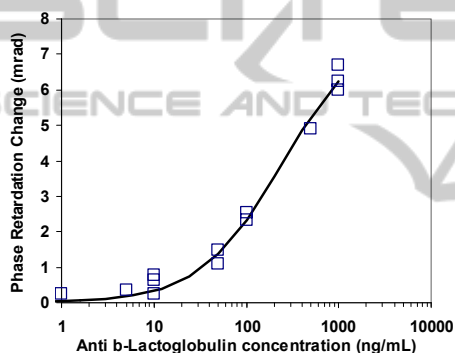


Figure 10: Phase retardation change upon injection of 2.5 nM SA-QD over biosensing experiments using a range of primary AB concentrations (5-1000ng/mL). The fitted line corresponds to a 1:1 binding model of K_D 228 ng/mL and R_{max} of 7.7 mrad.

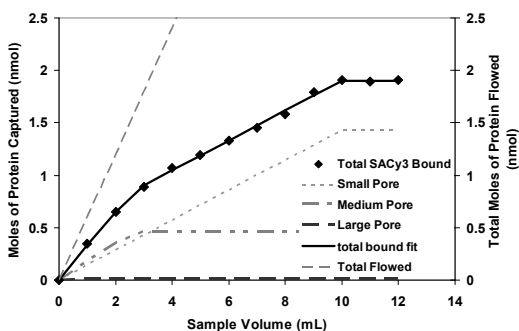


Figure 11: Amount of SA-Cy3 captured by biotinylated AAO membrane as a function of eluted sample volume. Lines show the fit to a mass transport to the membrane model with three pore sizes, assuming a fixed small pore size of 200nm at fitted 82.9% number density, 314nm at 17% and 1.4 μ m at 0.1%

ultimately limited by the demonstration of a distribution of pore sizes rather than the declared nominal pore diameter. The combination of porous membranes and SA-QD detection also raises the potential for other transduction mechanisms to be explored in these devices, such as fluorescence, colorimetric or back-pressure measurement.

5 DISCUSSION

Table 1: A comparison of the three principle sensors from the three EC projects along with the state of art.

Sensor	Volumetric LoD (RIU)	Protein mass LoD (pg/mm ²)	Protein concentration LoD	Response time	Time to result (mins)	Sample volume (ml)
SiN slot RR	5×10^{-6}	1	125 ng/ml	>300	>>60	5
SOI slot RR	4×10^{-5}	5	10 ng/ml	>300	>>60	5
Vernier RR	5×10^{-6}	NA	NA	>300	>>60	5
AAO Membrane	5×10^{-6}	?	34 ng/ml or 225pM	<1	<60	0.1
SOA	8×10^{-7}	?	60fM	<1	8	Small?

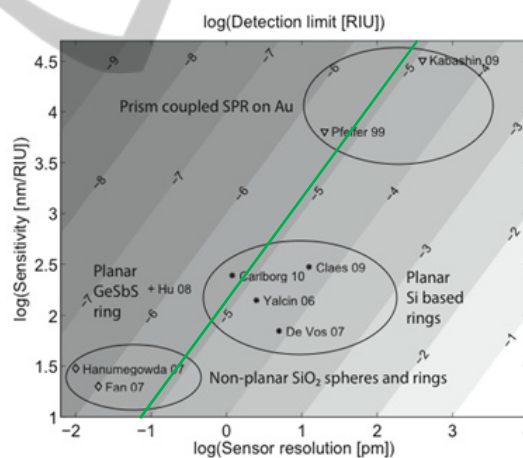


Figure 12: An analysis of the LoD from the principal sensor technologies within the three EC projects compared to others in the literature. The x-axis is the log of the wavelength resolution and the y-axis is the log of the device sensitivity in terms of wavelength shift per RIU. The grayscale then represents LoD 0. The SABIO sensor is labelled as Carlborg whilst the initial InTopsens sensor is labelled as Claes. A green continuous line on the graph represents the LoD of the Positive sensor. As the sensor uses a phase based measurement instead of wavelength, neither its sensitivity nor resolution can be plotted for a specific point.

When comparing the results from the principle sensor mechanisms used within the three EC projects one can see (Figure 12) their volumetric limits of detection are similar but still an order of magnitude below that of the state of art (SOA) for nanophotonic sensors (Iqbal, 2010).

Comparisons for protein mass or concentration LODs are difficult to make as they depend on the surface chemistry and exact protein used but all of three sensors are similar and inferior to the SOA. The POSITIVE sensor does however compare favourably with the SOA in terms of response time, size of sample and possibly time to result although the latter two are assay dependent making them difficult to compare especially given the lack of quantitative information for sample volumes used for the SOA results. It also probably has a far higher efficiency for analyte capture and if other transduction mechanisms were used simultaneously, it could have a far superior specificity, a very important parameter for many applications that rarely appears in academic publications.

6 CONCLUSIONS

In comparing various optical biosensors developed within three EC funded projects we have observed that firstly, they all have similar volumetric limits of detection, on the order of 10^{-6} RIU whereas limits of detection for proteomic assays vary and are difficult to compare with the data coming from different assays. It is noteworthy however that for the POSITIVE sensor total assay times were far less as were response times and minimum volumes of analyte necessary making it comparable at least in those regards to the state of art or nanophotonic sensors and interesting for certain applications.

Research in non-planar sensors, although currently facing more fabrication technology challenges than the planar types, can be expected to provide some very interesting results in the near future.

ACKNOWLEDGMENTS

As project manager of all three projects there are many contributors with whom I have worked directly and am most grateful for their efforts. I thank Jesus Alvarez, Hans Sohlström and Kristinn Gylfason for their photonics contributions in both SABIO and POSITIVE. Other direct contributors to the SABIO

work summarized here are Andrzej Kaźmierczak, Fabien Dortou, Laurent Vivien, Jon Popplewell, Gerry Ronan and Carlos A. Barrios. Other direct contributors to the INTOPSENS work summarized here include Tom Claes and Peter Bienstman. Further direct contributors from the POSITIVE project for article include Marcus J Swann, Laura Sola, Marina Cretich, Marcella Chiari and Tormod Volden. As I review the collaborative projects SABIO, INTOPSENS and POSITIVE, many others have contributed.

REFERENCES

- X. Fan, I. M. White, S. I. Shopova, H. Zhu, J. D. Suter, and Y. Sun. (2008). Sensitive optical biosensors for unlabeled targets: A review, *Anal. Chim. Acta*, 620, (1/2), p8–p26.
- D. Hill. (2011). Advances in nanophotonic sensing technologies during three international label-free lab-on-chip projects, *BioNanoScience*, 1, p162–p172.
- D. Janasek, J. Franzke, and A. Manz. (2006). Scaling and the design of miniaturized chemical-analysis systems, *Nature* 442, p374–p380.
- F. S. Ligler, (2009). Perspective on optical biosensors and integrated sensor systems, *Anal. Chem.*, 81, (2), p519–p526.
- A. Brecht and G. Gauplitz. (1995). *Biosensors and Bioelectronics*, 10, p923–p936.
- D. Markov, D. Begari and D. J. Bornhop. (2002). Breaking the 10^{-7} Barrier for RI Measurements in Nanoliter Volumes, *Anal. Chem.*, 74, p5438–p5441.
- K. Zinoviev, L. G. Carrascosa, J. Sánchez del Río, B. Sepúlveda, C. Domínguez, and L. M. Lechuga. (2008). Silicon photonic biosensors for lab-on-a-chip applications, *Advances in Optical Technologies*, p383927.1–p383927.6.
- J. A. De Feijter, J. Benjamins and F. A. Veer. (1978). Ellipsometry as a tool to study the adsorption behavior of synthetic and biopolymers at the air-water interface, *Biopolymers* 17, (7), p1759–p1772.
- K. Tiefenthaler, and W. Lukosz. Integrated optical switches and gas sensors, (1984). *Opt. Lett.* 9, p137–p139.
- W. Lukosz, and K. Tiefenthaler. (1988). Sensitivity of integrated optical grating and prism couplers as (bio)chemical sensors, *Sensors and Actuators* 15, (3), p273–p284..
- K. Tiefenthaler, and W. Lukosz. (1989). Sensitivity of grating couplers as integrated optical chemical sensors, *J. OSA B: Opt. Phys.* 6, (2), p209–p220.
- V. R. Almeida, Q. Xu, C. A. Barrios, and M. Lipson. (2004). Guiding and confining light in void nanostructure, *Opt. Lett.* 29, (11), p1209–p1211.
- Q. Xu, V. R. Almeida, R. R. Panepucci, and M. Lipson. (2004). Experimental demonstration of guiding and confining light in nanometer-size low-refractive-index material, *Opt. Lett.*, 29 (14), p1626–p1628.

- H. Sohlström, K. Gylfason, D. Hill. (2010). Real-time label-free biosensing with integrated planar waveguide ring-resonators. *Proc. SPIE* 7719, 77190B.
- Gylfason, K. G., Carlborg, C. F., Kazmierczak, A., Dortu, F., Sohlström, H., Vivien, L., Barrios, C. A., van der Wijngaart, W., and Stemme, G., "On-chip temperature compensation in an integrated slot-waveguide ring resonator refractive index sensor array", *Opt. Expr.* 18(4), 3226–3237 (2010).
- C. F. Carlborg, K. B. Gylfason, A. Kamierczak, F. Dortu, M. J. Bañuls Polo, A. Maquieira Catala, G. M. Kresbach, H. Sohlström, T. Moh, L. Vivien, J. Popplewell, G. Ronan, C. A. Barrios, G. Stemme, and W. van der Wijngaart. (2010). A packaged optical slot-waveguide ring resonator sensor array for multiplex label-free assays in labs-on-chips. *Lab Chip*. 10, p281–p290.
- A. Kazmierczak, F. Dortu, O. Schrevels, D. Giannone, L. Vivien, D. M. Morini, D. Bouville, E. Cassan, K. G. Gylfason, H. Sohlström, B. Sanchez, A. Griol, and D. Hill. (2009) Light coupling and distribution for Si₃N₄/SiO₂ integrated multichannel single-mode sensing system. *Opt. Eng.* 48, (1), 014401.
- K. De Vos, I. Bartolozzi, E. Schacht, P. Bienstman, and R. Baets. (2007). Silicon-on-insulator microring resonator for sensitive and label-free biosensing. *Opt. Expr.* 15, (12), p7610–p7615.
- T. Claes, J. G. Molera, K. De Vos, E. Schacht, R. Baets, and P. Bienstman. (2009) Label-free biosensing with a slot-waveguide-based ring resonator in silicon on insulator. *J. IEEE Photonics* 1, (3), p197–p204.
- T. Claes, W. Bogaerts, and P. Bienstman. (2010). Experimental characterization of a silicon photonic biosensor consisting of two cascaded ring resonators based on the Vernier-effect and introduction of a curve fitting method for an improved detection limit. *Optics Express*, 18, (22), p22747.
- T. D. Lazzara, I. Mey, C. Steinem, A. Janshoff. (2011). Benefits and limitations of porous substrates as biosensors for protein adsorption, *Anal. Chem.*, 83, (14), p5624-p5630.
- M. M. Orosco, C. Pacholski, M.J. Sailor. (2009). Real-time monitoring of enzyme activity in a mesoporous silicon double layer. *Nature Nanotechnology*, 4, p255.
- C. K. Tsang, T. L. Kelly, M. J. Sailor, Y. Y. Li, (2012). Highly Stable Porous Silicon–Carbon Composites as Label-Free Optical Biosensors. *ACS Nano*, 6, p10546.
- S.D. Alvarez, C. P. Li, C. E. Chiang, I. K. Schuller, M. J. Sailor. (2009). A Label-Free Porous Alumina Interferometric Immunosensor. *ACS Nano*, 3, p3301.
- T. Kumeria, M. D. Kurkuri, K. R. Diener, L. Parkinson, D. Losic, (2012). Label-free reflectometric interference microchip biosensor based on nanoporous alumina for detection of circulating tumour cells. *Biosensors and Bioelectronics*, 35, (1), 167.
- T. Kumeria, D. Losic, (2012). Controlling interferometric properties of nanoporous anodic aluminium oxide” *Nanoscale Research Letters*, 7, (88), p1.
- A. A. Yanik, M. Huang, A. Artar, T. Y. Chang, H. Altug. (2010). Integrated nanoplasmonic-nanofluidic biosensors with targeted delivery of analytes. *Applied Physics Letters*, 96, (2), p021101.
- Y. Guo, H. Li, K. Reddy, H.S. Shelar, V.R. Nittoor, X. Fan. (2011). Optofluidic Fabry-Perot cavity biosensor with integrated flow-through micro-/nanochannels. *Applied Physics Letters*, 98, (4), p041104.
- J. Álvarez, P. Bettotti, I. Suárez, N. Kumar, D. Hill, V. Chirvony, L. Pavesi, J. Martínez-Pastor. (2011). Birefringent porous silicon membranes for optical sensing. *Opt. Express*, 19, (27), p26106.
- J. Álvarez, P. Bettotti, N. Kumar, I. Suarez, D. Hill, J. Martínez-Pastor. (2012). Highly-sensitive anisotropic porous silicon based optical sensors. *Proc. SPIE*, 8212, (1), p821209.
- J. Álvarez, L. Sola, G. Platt, M. Cretich, M. Swann, M. Chiari, D. Hill, and J. Martínez-Pastor. (2013). Real-time polarimetric biosensing using macroporous alumina membranes. *Proc. SPIE* 8765, Bio-MEMS and Medical Microdevices, p876501.
- J. Álvarez, L. Sola, M. Cretich, M. J. Swann, K. B. Gylfason T. Volden, M. Chiari, D. Hill. (2014). Real time optical immunosensing with flow through porous alumina membranes. *Journal of Sensors and Actuators B*, 202, p834-p839.
- G. W. Platt, F. Damin, M. J. Swann, I. Metton, G. Skorski, M. Cretich, M. Chiari. (2014). Allergen immobilisation and signal amplification by quantum dots for use in a biosensor assay of IgE in serum. *Biosensors and Bioelectronics*, 52, p82–p88.
- M. Cretich, D. Breda, F. Damin, M. Borghi, L. Sola, S.M. Unlu, & M. Chiari. (2010). Allergen microarrays on high sensitivity silicon slides. *Analytical and bioanalytical chemistry*, 398, (4), p1723-p1733.
- L. Sola, J. Álvarez, M. Cretich, M. J. Swann, T. Volden, M. Chiari, D. Hill. (2015). Characterisation of porous alumina membranes for efficient, real-time, flow through biosensing. *J. Membrane Science*, 276, p128–p135.
- J. Álvarez, C. Serrano, D. Hill, and J. Martínez-Pastor. (2013). Real-time polarimetric optical sensor using macroporous alumina membranes. *Opt. Lett.* 38, (7), p1058-p1060.
- M. Iqbal, M. A. Gleeson, B. Spaugh, F. Tybor, W. G. Gunn, M. Hochberg, T. Baehr-Jones, R. C. Bailey, and L. C. Gunn. (2010). Label-Free Biosensor Arrays Based on Silicon Ring Resonators and High-Speed Optical Scanning Instrumentation. *IEEE Journal of Selected Topics In Quantum Electronics*, 16, (3).
- K. B. Gylfason, (2010). Integrated Optical Slot-Waveguide Ring Resonator Sensor Arrays for Lab-on-Chip Applications. *PhD Thesis* TRITA-EE 2010:012, KTH-Royal institute of Technology, Stockholm.